Research paper

Exosomes combined with biosynthesized cellulose conduits improve peripheral nerve regeneration

Tian-Wei Cui [a,b,1], Li-Fang Lu [a,b,1], Xu-Dong Cao [c], Quan-Peng Zhang [a,b], Yue-Bin He [a], Ya-Ru Wang [a], Rui Ren [a,b], Xin-Yu Ben [a], Pan-Li Ni [a], Zhi-Jian Ma [a,b], Yun-Qing Li [d], Xi-Nan Yi [a,b,*], Ren-Jun Feng [a,b,*]

[a] Key Laboratory of Brain Science Research and Transformation in Tropical Environment of Hainan Province, Hainan Medical University, Haikou, China
[b] Department of Human Anatomy, Hainan Medical University, Haikou, China
[c] Department of Chemical and Biological Engineering, University of Ottawa, Ottawa, Ontario, Canada
[d] Department of Anatomy, Histology and Embryology and K.K. Leung Brain Research Centre, The Fourth Military Medical University, Xi'an, China

ARTICLE INFO

ABSTRACT

Peripheral nerve injury is one of the more common forms of peripheral nerve disorders, and the most severe type of peripheral nerve injury is a defect with a gap. Biosynthetic cellulose membrane (BCM) is a commonly used material for repair and ligation of nerve defects with gaps. Meanwhile, exosomes from mesenchymal stem cells can promote cell growth and proliferation. We envision combining exosomes with BCMs to leverage the advantages of both to promote repair of peripheral nerve injury. Prepared exosomes were added to BCMs to form exosome-loaded BCMs (EXO-BCM) that were used for nerve repair in a rat model of sciatic nerve defects with gaps. We evaluated the repair activity using a pawprint experiment, measurement and statistical analyses of sciatica function index and thermal latency of paw withdrawal, and quantitation of the number and diameter of regenerated nerve fibers. Results indicated that EXO-BCM produced comprehensive and durable repair of peripheral nerve defects that were similar to those for autologous nerve transplantation, the gold standard for nerve defect repair. EXO-BCM is not predicted to cause donor site morbidity to the patient, in contrast to autologous nerve transplantation. Together these results indicate that an approach using EXO-BCM represents a promising alternative to autologous nerve transplantation, and could have broad applications for repair of nerve defects.

1. Introduction

Peripheral nerve injury remains one of the most challenging clinical problems and causes substantial patient suffering as well as economic burden (Li et al., 2021). The most serious form of nerve injury is a nerve defect involving gaps (Wang et al., 2022). In the absence of a primary suture, suitable interfascicular autologous and allogeneic nerve grafting to repair both short and long defects remains the gold standard method (Hazer Rosberg et al., 2021). However, this approach is constrained by donor site morbidity with the possibility of neuroma growth at both repair site and graft site as well as graft availability and possibility of immunological rejection (Sun et al., 2019). To overcome these obstacles, numerous different types of bioengineered nerve conduits have been introduced and characterized in experimental nerve injury models

(Hazer Rosberg et al., 2021) including poly-3-hydroxyoctanoate (Hazer et al., 2013), poly-3-hydroxybutyrate (Sakar et al., 2014), poly (ε-caprolactone) (Niu et al., 2014), chitosan (Meyer et al., 2016), and cellulose (Stumpf et al., 2020; Stumpf et al., 2018).

Biosynthesized cellulose (BC) is promoted as a viable alternative to autografts and has been demonstrated to have various desirable features, including exceptional stability, high mechanical strength, and good biocompatibility (Stumpf et al., 2018). BC has been investigated for use in vascular grafts (Samfors et al., 2019), urinary repair (Lv et al., 2018) and for artificial corneas (Zhang et al., 2020), as well as regeneration of cartilage (Xun et al., 2021), bone (Dubey et al., 2021), and nerves (Hou et al., 2018; Stumpf et al., 2020). These studies demonstrated that BC was completely absorbed into the host tissue and caused no inflammation or rejection reactions (Dubey et al., 2021; Lv et al.,

2018; Samfors et al., 2019; Stumpf et al., 2020; Xun et al., 2021; Zhang et al., 2020).

To further enhance the regeneration capacity of nerve conduits, biomaterials are often applied with neurotrophic factors (Powell et al., 2021) such as glial cell-derived neurotrophic factor (GDNF), brain-derived neurotrophic factor (BDNF) and neurotrophin-3 (NT3) (Dervan et al., 2021). Several reports have described the repair of peripheral nerve defects with exosomes combined with biomaterials. Exosomes play a significant role in intercellular communication based on the active cargo components they carry including proteins, lipids, metabolites, and nucleic acids (Kalluri and LeBleu, 2020). Stem cell exosomes can promote peripheral nerve regeneration (Zhao et al., 2020) and provide central nerve neuroprotection (Kalluri and LeBleu, 2020; Wen et al., 2022). MicroRNAs (miRNAs) contained in exosomes play important roles in many physiological and pathological processes. MiRNA-340 positively regulated cell debris removal at the injury site and axon growth in vivo (Bischoff et al., 2022). MiRNA-21 derived from exosomes has the ability to promote cell regeneration, which can promote axonal regeneration via phosphatase and tensin homologue deleted on chromosome 10 (PTEN) downregulation and phosphoinositide 3 (PI3)-kinase activation in neurons (López-Leal et al., 2020). MiRNA-181 plays a major role in inhibiting neuroinflammation and regulating the phenotype of microglia (Wen et al., 2022). Additionally, exosomes may contain neurotrophic factors that promote the regeneration of peripheral nerves.

The aim of this study was to design exosome-incorporated BC membranes (EXO-BCMs) to induce peripheral nerve regeneration in a rat model of sciatic nerve injury. To examine the biosafety and characteristics of EXO-BCM, interdisciplinary approaches were used to assess biocompatibility, biodegradability, and repair activity of the graft. Results of this study may pave the way for the use of EXO-BCM to repair peripheral nerve injuries.

2. Materials and methods

2.1. Manufacturing of chitosan

BCMs were synthesized by bacterial fermentation (Stumpf et al., 2013). A stock culture of *Gluconacetobacter hansenii* ATCC 53582 was inoculated into culture medium consisting of mannitol (25 g/L), yeast extract (5.0 g/L), and peptone (3.0 g/L) and then incubated on culture plates at 30 ℃ for seven days. BCMs were taken from the plates and washed with distilled water before immersion in 0.1 M NaOH at 50 ℃ for 24 h, followed by consecutive rinses with distilled water until a neutral pH was reached. After autoclaving, BCMs were stored at 4 ℃ until use.

2.2. Animals

Sprague-Dawley (SD) rats (6 weeks-old) were purchased from Changsha Tianqin Biotechnology Co., Ltd. The rats were raised and bred according to Hainan Medical University regulations, and second generation animals were raised for around one month prior to use. Six of the second generation animals were used to prepare adipose-derived mesenchymal stem cells, and the remainder were used for sciatic nerve injury repair experiments. All experimental protocols were approved by the Clinical Research and Laboratory Animal Ethics Committee of Hainan Medical University (approval no. HYLL-2017–036).

2.3. Exosomes

2.3.1. Adipose tissue-derived mesenchymal stem cell (ADMSC) culture
P1 rat ADMSCs isolated according to a previously described protocol were used (Bandeira et al., 2018). ADMSCs were expanded in alpha-minimum essential medium (a-MEM) (Thermo Fisher Scientific, USA), supplemented with 10 % fetal bovine serum (Thermo Fisher Scientific, USA) and 1 % (by volume) penicillin-streptomycin mixture (Thermo Fisher Scientific, USA), and incubated in flasks for 72 h at 37 ℃ in a humidified atmosphere with 5 % CO_2. Upon reaching 80 % confluence, the cells were passaged with 0.25 % trypsin-EDTA solution (Thermo Fisher Scientific, USA). After passage 5 times, the cells were collected for exosome isolation.

2.3.2. Exosome extraction and identification
ADMSCs were washed with phosphate buffered saline (PBS) and subsequently cultured in serum-free medium for 72 h at 37 ℃ and 5 % CO_2. To enrich the exosomes, the sample was sequentially centrifuged at 300g for 10 min, 2000g for 20 min, and 10,000g for 30 min before passage through a 0.22 μm filter, and centrifugation at 100,000g for 80 min. The pellet was resuspended in PBS and ultracentrifuged once before again resuspending in PBS to generate an exosome solution for future use. Exosome size and concentration were assessed using nanoparticle tracking analysis (NTA) with a Zeta View® system (Particle Metrix, Germany). NTA illuminates exosomes with a laser beam and captures the scattered light with a high-resolution camera, allowing researchers to visualize and quantify the motion of each individual exosome. By analyzing the diffusion coefficient of exosomes, NTA can accurately determine their hydrodynamic diameter. Additionally, by measuring the light intensity of each particle, NTA can also precise calculate the concentration of exosomes in the sample. Exosome morphology was captured with a transmission electron microscope (Hitachi, Japan) operated at 60 kV.

2.4. Exosome-incorporated BCMs

To facilitate subsequent nerve defect repair surgery, a hole was punched in each of the four corners of the BCMs. After autoclaving, the BCMs were dried to remove residual moisture. Then, 4 μL sterile exosome solution (1.9×10^8 exosomes per μL) was slowly and uniformly dripped onto the BCMs to form EXO-BCMs that were stored under sterile conditions at 4 ℃ until use.

2.5. Experimental design and treatments

Healthy adult male SD rats weighing 180–200 g were divided into 6 groups with 6 rats in each group. In the Autologous nerve group (AUT), severed nerves were bridged using autologous nerves. In the Autologous nerve + gastrocnemius [EXO] group (AUT+GAS[EXO]), severed nerves were connected using autologous nerves before injection of exosomes into the gastrocnemius. In the EXO-BCM group (EXO-BCM), severed nerves were joined using EXO-BCMs. In the BCM + gastrocnemius [EXO] group (BCM+GAS[EXO]), severed nerves were linked using BCMs before the gastrocnemius was injected with exosomes. In the BCM group (BCM), BCMs were used to connect the severed nerves. Lastly, in the fascia group (FAS), fascia was used to bridge the severed nerves.

2.5.1. Nerve removal surgery
Rats were anesthetized by injection of 10 % chloral hydrate (0.3 ml per 100 g body weight) into the abdominal cavity. The anesthetized animal was then fixed on a board in a prone position. The fur on the lower edge of the piriformis of the right thigh was shaved and the exposed skin was sterilized three times with alcohol. An oblique incision was made in the right hip with a scalpel under sterile conditions, and the gluteal muscle was bluntly dissected to expose the right sciatic nerve. After finding the sciatic nerve trunk, ophthalmic scissors were used to cut out 5 mm of the sciatic nerve. This study deviates from the conventional 10 mm length in order to establish the experimental methodology and set the groundwork for subsequent experiments involving the 10 mm defect size.

2.5.2. Bridging surgery
Autologous nerve bridging: After inverting the 5 mm cut of the

sciatic nerve trunk, the epineurium of the two cut ends of the sciatic nerve trunk was sutured with biodegradable and bioabsorbable surgical sutures under an operating microscope. The skin wound was sutured and disinfected with alcohol.

BCM Bridging: A conduit-like roll was formed by wrapping and then suturing the two cut ends of the sciatic nerve in a BCM (approximately 1 cm wide and 2 cm long). The middle of the BCM roll, with an internal diameter of approximately 0.30 cm and a thickness of 0.08 mm, was sutured to prevent spreading. Finally, the wound was sutured and sterilized.

Fascial bridging: A section of fascia approximately 2 mm wide and 5 mm long was sutured to the sciatic nerve trunk epineurium. The wound was then disinfected.

2.5.3. Administration

Immediately after the operation, 2 μL exosomes (1.9×10^8 exosomes/μL) was injected into the right gastrocnemius in AUT+GAS^{EXO} and BCM+GAS^{EXO} groups and then again after 3 days. After administering the injection for 5 min, the needle was left in place for an additional 5 min to ensure complete absorption of the liquid, and then it was carefully withdrawn.

2.6. Behavioral analysis

2.6.1. Behavioral presentation assessment

Recovery of right hindlimb locomotor activity was monitored by analysis of the free walking pattern. A walking track analysis was performed at 24 h after surgery and then 4 and 8 weeks later (de Medinaceli et al., 1982). A self-made rat pawprint walking channel was used for walking track testing, and the white paper of the channel substrate was used to record pawprints after inking of the paws.

2.6.2. Sciatica function index (SFI)

SFI values for the rats were measured based on the above-mentioned rat pawprints. Three variables were measured according to the pawprints made by the experimental side paw (E) and the untreated, normal side paw (N). Print length (PL) represents the distance between the heel and the top of the third toe, and toe spread (TS) represents the length from the first toe to the fifth toe. Intermediary toe spread (IT) is the distance from the second toe to the fourth toe. Several prints made by each paw were obtained from the experimental and normal sides on each track. The formula for calculation is: SFI = −38.3(EPL − NPL)/NPL + 109.5(ETS − NTS)/NTS + 13.3(EIT − NIT)/NIT − 8.8. SFI = 0 represents normal function, while SFI = −100 represents complete nerve disconnection.

2.6.3. Paw withdrawal thermal latency (PWTL)

PWTL testing was performed with an RB-200 intelligent hot plate (Chengdu Techman, China) according to the manufacturer instructions to detect thermal hyperalgesia upon radiant heat stimulation. The duration from the start of application to withdrawal of the paw was recorded using a digital timer.

2.7. Immunohistochemistry and morphometry

At 8 weeks after surgery, the implanted nerve grafts were excised. The regenerated nerves at the distal end were fixed in 4 % paraformaldehyde for 24 h, washed in water overnight, dehydrated via ethanol gradient, cleared in xylene, embedded in paraffin and sectioned into 5 μm-thick slices. For immunohistochemistry analysis, slices were deparaffinized, rehydrated, blocked with hydrogen peroxide, and subjected to heat-induced antigen retrieval. The sections were blocked against non-specific binding with goat serum for 1 h, and incubated with primary antibodies against S100 overnight at 4 ℃ followed by a one-hour incubation with secondary antibody diluted 1:300. The slices were stained using a 3,3'-diaminobenzidine (DAB) kit (Merck, USA),

counterstained with hematoxylin, dehydrated, and mounted. For morphometry analysis, sections were deparaffinized and rehydrated with an ethanol gradient, and then stained for 30 min in 0.1 % aqueous toluidine blue. The slices were differentiated with 0.5 % glacial acetic acid until the nuclei were clear. The sections were washed, dehydrated, cleaned in xylene and mounted.

2.8. Regenerated nerve fiber count

Images were captured using an inverted microscope (Leica Microsystems, UK) under uniform lighting conditions. To avoid observer bias, a blinded investigator quantified all of the sections. Parameters for regenerated nerve fibers including average diameter and density of nerve fibers were quantified by Image J software.

2.9. Statistical analysis

All data are expressed as the mean ± standard deviation and were analyzed with GraphPad Prism software (Dotmatics, USA). Statistical analyses included one-way analysis of variance (ANOVA) followed by Tukey's test for multiple comparisons. A probability (P) value less than 0.05 (P < 0.05) was considered to be a statistically significant difference.

3. Results

3.1. Exosome characterization

SD rat ADSCs grow in clusters having a fusiform shape, which appears as a relatively irregular arrangement under a microscope (Fig. 1A, B). With transmission electron microscopy, exosomes derived from ADSCs presented as irregular ellipses (Fig. 1C, D). Detection using a NTA showed a median exosome particle size of 118.6 nm at a concentration of 1.9×10^{11}/ml (Fig. S1).

3.2. Observation of behavioral presentation to assess nerve repair

To monitor recovery of right hindlimb motor activity, behavioral analysis was performed 24 h and 4 and 8 weeks after surgery to repair sciatic nerve defects. The paws of the rats were inked and the ink was transferred to white paper as the animal passed through a walking channel. Pawprints measured 24 h after surgery were not clearly defined and the prints of each toe were not separate (data not shown). At 4 weeks after surgery, the clarity of the pawprints and their respective sizes was higher for animals in groups AUT and AUT+GAS^{EXO} compared to the 24 h time point and covered a larger area relative to prints made by animals in the EXO-BCM, BCM+GAS^{EXO}, BCM, and FAS groups. Additionally, animals in the AUT and AUT+GAS^{EXO} groups exhibited the earliest partial separation of time the pawprints and toes (data not shown). At 8 weeks after surgery, the clarity of toe contours and paw area for the AUT and AUT+GAS^{EXO} groups were superior to those for the EXO-BCM group, which itself was superior to that for the BCM+GAS^{EXO} group. The BCM and FAS groups had the poorest clarity and smallest area of the groups (Fig. 2A).

These results of behavioral experiments indicate that: 1) From a temporal perspective, nerve injury repair occurs over a long period and within a certain time range; the repair effect improved with longer times after surgery; and 2) From an inter-group perspective, autologous nerve transplantation, as expected as the gold standard for peripheral nerve injury repair, had the best repair effect for sciatic nerve defects. The second-best repair effect was seen for EXO-BCM.

3.3. SFI values to assess nerve repair

We next measured SFI values to quantify recovery of right hind limb motor activity. No significant differences in SFI (p > 0.05) were observed among the experimental groups 24 h after the surgery
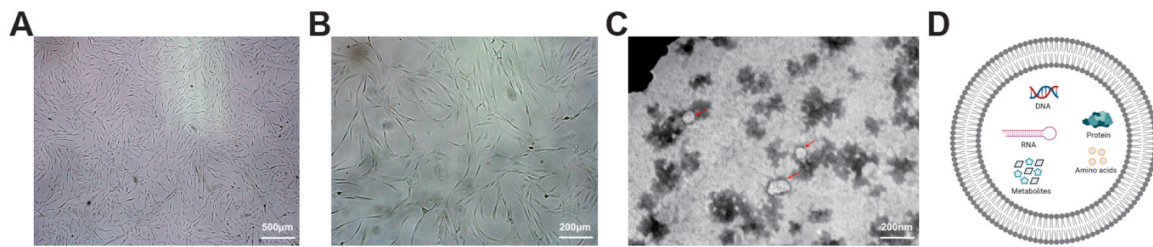
Fig. 1. Identification of exosomes derived from ADSCs. Morphology of ADSCs under (A) 4x and (B) 10x magnification (scale bar, 500 μm and 200 μm, respectively). (C) Morphology of exosomes as observed with transmission electron microscopy. Scale bar, 200 nm. (D) Schematic illustration of exosomes.

(Fig. 2B). The SFI values at 4 weeks after surgery relative to those at 24 h suggested that a certain degree of nerve injury repair occurred in each group (Fig. 2C). Analysis of the SFI values showed that the AUT+GAS^{EXO} group was significantly superior to the AUT group ($P < 0.001$), which was significantly superior to the EXO-BCM group ($P < 0.001$). These two groups were significantly superior to the BCM+GAS^{EXO} ($P < 0.05$), BCM ($P < 0.01$) and FAS ($P < 0.001$) groups. At 8 weeks after surgery, the SFI values for all groups were significantly higher than those at 4 weeks after surgery. The repair effect at 4 and 8 weeks was similar between groups, except that at 8 weeks the difference between the AUT and AUT + GAS^{EXO} groups was smaller than at 4 weeks and there was no significant difference in SFI values for the EXO-BCM and BCM + GAS^{EXO} groups (Fig. 2D). As the time after surgery increased, the repair effect seen for the two groups treated with BCM (i.e., EXO-BCM and BCM+GAS^{EXO}), and especially the EXO-BCM group, was close to that for autologous nerve transplantation at 8 weeks after surgery (Fig. 2E, F).

These results suggest that exosomes function to promote repair of sciatic nerve defects. EXO-BCM can represent an effective alternative to repair peripheral nerve defects if autogenous nerve transplantation, the gold standard to treat long segment nerve defects, cannot be carried out.

3.4. PWTL values to assess nerve repair

We utilized PWTL testing to assess pain sensitivity in rats as a measure of the extent of neural connection repair of sciatic nerve defects. There was no significant difference in PWTL values among the groups at 0 h before surgery (Fig. 3A). At 24 h after surgery, the AUT group and AUT+GAS^{EXO} group had significant improvement in PWTL compared to the EXO-BCM, BCM+GAS^{EXO}, and BCM groups, which were all significantly better than the FAS group. PWTL values did not significantly differ between the AUT group and the AUT+GAS^{EXO} group, or among the EXO-BCM, BCM+GAS^{EXO}, and BCM groups (Fig. 3B). At week 8, the perception of animals in each group was largely restored, and there was a significant difference in PWTL values between any two groups ($P < 0.001$) (Fig. 3C). In terms of perceptual function recovery, the nerve repair activity of AUT+GAS^{EXO} and AUT groups was the best, and was close to the preoperative sensory perception level, followed, in order, by EXO-BCM, BCM+GAS^{EXO}, and BCM. FAS had the worst repair effect, and after 8 weeks the perception was close to that at 24 h after surgery (Fig. 3D, E). This result demonstrates that exosomes promote repair of sciatic nerve defects, and, next to autologous nerve transplantation, EXO-BCM is the best choice for repairing peripheral nerve defects.

3.5. Assessment of nerve repair according to quality and quantity of regenerated nerve fibers

To assess the morphology, quantity, and diameter of repaired nerve fibers, sections of the regenerated nerve fibers with toluidine blue staining and DAB + hemataoxylin staining were observed with histological light microscopy. The number of regenerated myelinated fibers was counted at the experimental endpoint (i.e., 8 weeks after surgery) At 8 weeks after surgery, the AUT group and AUT+GAS^{EXO} group had the highest number of regenerated myelinated fibers that had a neat arrangement and thick myelin sheath at the distal end of the sciatic nerve injury. Animals in the EXO-BCM and BCM+GAS^{EXO} groups had relatively high numbers of regenerated nerve fibers, but the distribution was less even and the arrangement less regular than that seen for groups with autologous treatment. The BCM group had relatively few regenerated nerve fibers, which also had an uneven distribution and irregular arrangement. The FAS group had the fewest regenerated nerve fibers and those that were present had a very irregular arrangement (Fig. 4A, B). Overall, the AUT+GAS^{EXO} group had the most regenerated nerve fibers, and the count was significantly higher than that for the AUT group, as well as for the EXO-BCM and BCM+GAS^{EXO} groups. The number of fibers in samples from animals in the EXO-BCM and the BCM+GAS^{EXO} groups did not significantly differ. These four groups had significantly more fibers than the BCM group, and animals in the FAS group had the fewest fibers (Fig. 4C).

The trend for the diameter of regenerated nerve fibers was similar to that for the number of regenerated nerve fibers (Fig. 4D). Taken together, these results support a role for exosome function to promote the repair of sciatic nerve defects, and that EXO-BCM has the best activity for repair of peripheral nerve defects after autologous nerve transplantation.

4. Discussion

Neurotmesis is the most severe type of peripheral nerve injury. For neurotmesis involving gaps larger than 5 mm, the likelihood of complete axonal regeneration and functional recovery is low. Therefore, this type of injury often leads to paralysis (Wang et al., 2022). When neurotmesis occurs, grafts can be needed to restore continuity and support nerve fiber growth (Li et al., 2021). Although autologous nerve transplantation is considered as the gold standard treatment for these cases, there are some disadvantages with this approach such as insufficient supply of donor nerve (Wang et al., 2022). Developing viable and compelling alternative treatments to autologous nerve grafts remains a critical challenge for researchers interested in peripheral nerve defect repair (Li et al., 2021). Animal models of sciatic nerve defects having gaps >5 mm have thus been used to mimic human neurotmesis (Wang et al., 2022). In this study, we successfully constructed a rat model of sciatic nerve defect that has a defect of up to 5 mm. Moreover, we evaluated the effectiveness of EXO-BCM in repairing the sciatic nerve defect in this rat model. Expanding on the methodology established in this experiment, our next research phase will focus on investigating the repair potential of EXO-BCM for a 10 mm sciatic nerve defect.

BC is considered to be a viable alternative to autologous grafts and has several desirable characteristics, including excellent stability, high mechanical strength, and good biocompatibility (Stumpf et al., 2020; Stumpf et al., 2018). Here we utilized BCMs as a material for bridging nerve stumps, with the expectation of its ability to connect severed nerves. To achieve satisfactory repair of sciatic nerve defects, simply reconnecting the two severed nerve ends is not sufficient (Powell et al., 2021). Substances that protect and promote nerve growth, such as GDNF, BDNF and NT3 (Dervan et al., 2021), are also required, as are
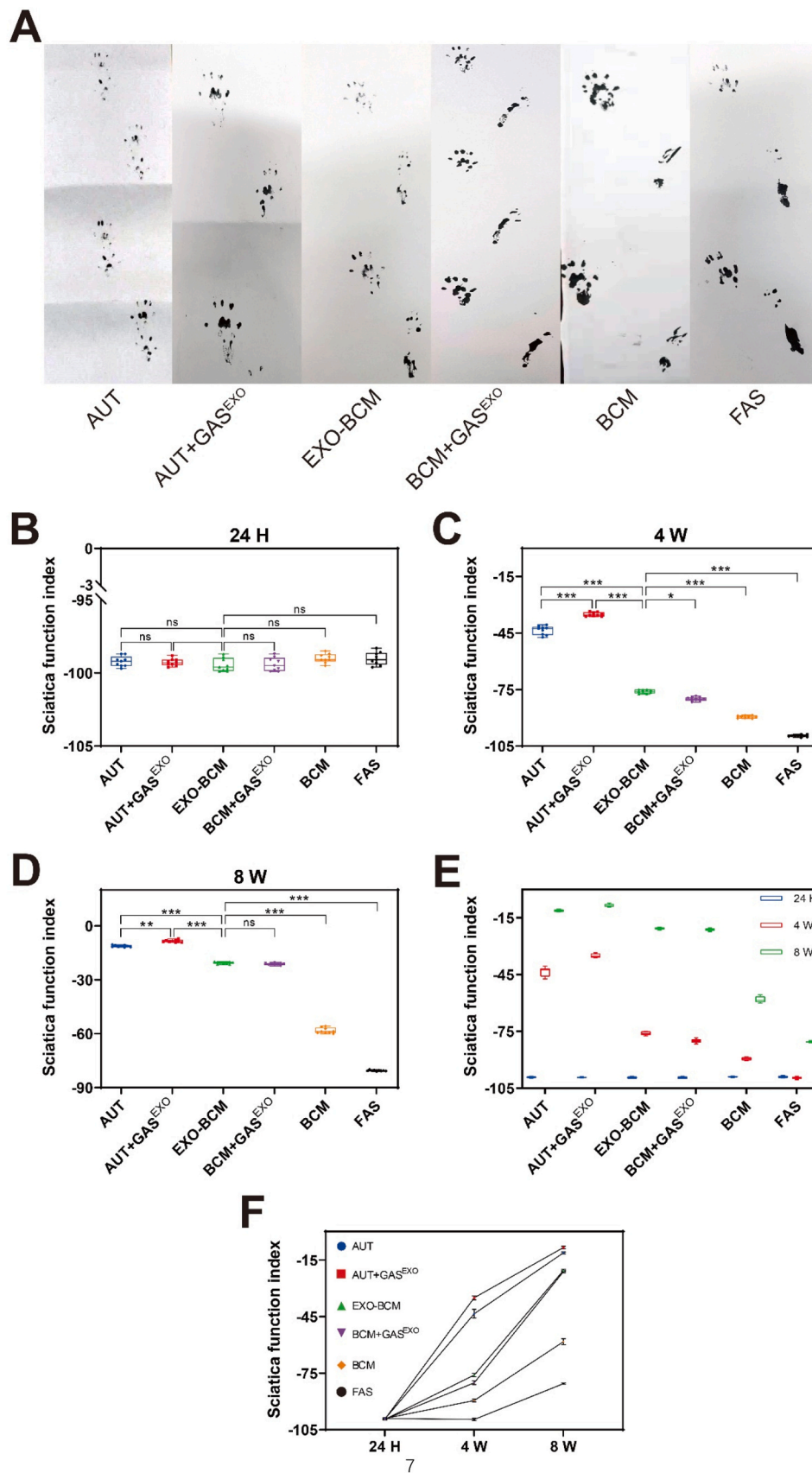
Fig. 2. Pawprints and sciatica function index (SFI) of experimental rats. (A) Pawprints for all groups 8 weeks after surgery. Left: normal foot (control), right: surgical foot. SFIs for all groups (B) 24 h, (C) 4 weeks and (D) 8 weeks after surgery. Trend in SFI changes (E) among the groups and (F) over time. n = 9, * adjusted P values between 0.05 and 0.01, ** adjusted P values between 0.01 and 0.001, *** adjusted P values P < 0.001.
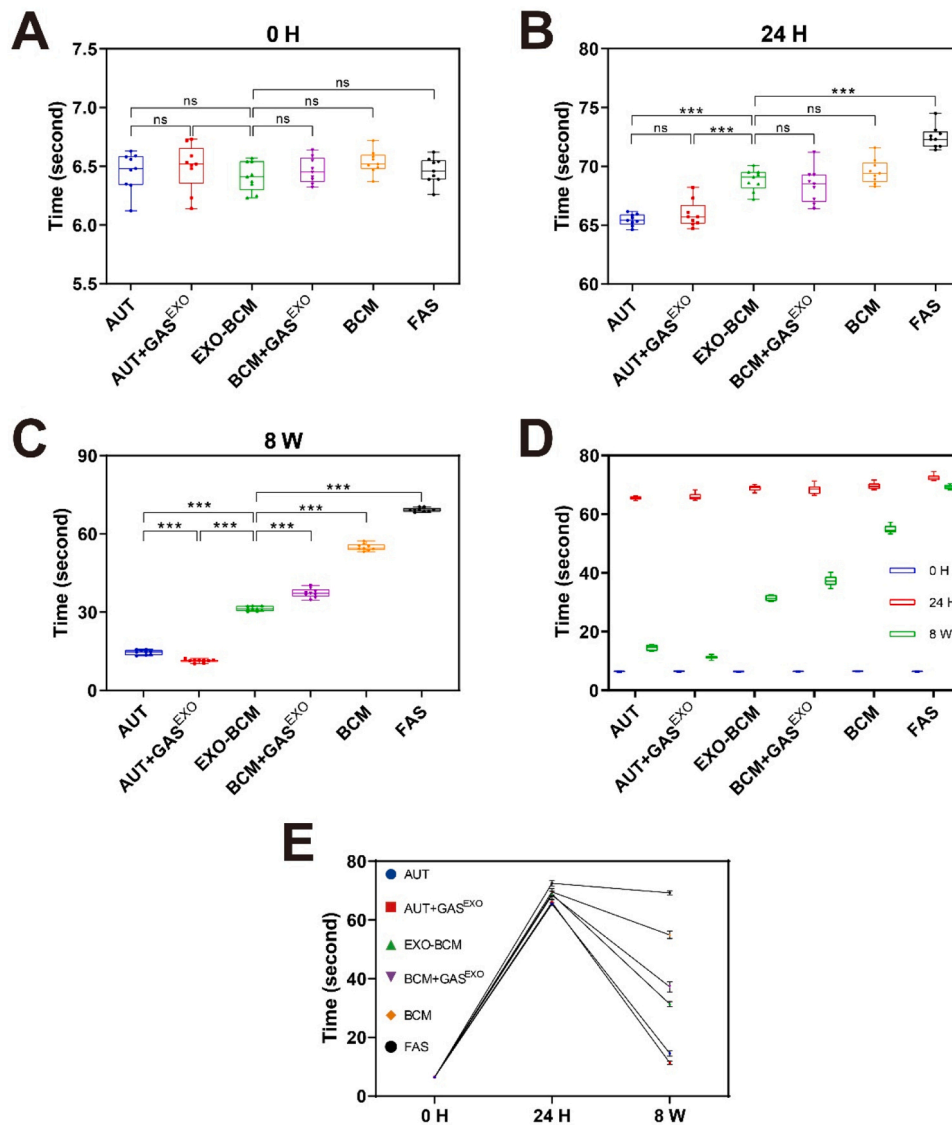
Fig. 3. Paw withdrawal thermal latency (PWTL) values for different experimental groups. PWTL values for all groups at (A) 0 h (B) 24 h and (C) 8 weeks after surgery. (D) The change in trends of PWTL value for (D) different experimental groups and (E) over time. n = 9, * adjusted P values between 0.05 and 0.01, ** adjusted P values between 0.01 and 0.001, *** adjusted P values P < 0.001.

exosomes (Kalluri and LeBleu, 2020; Wen et al., 2022; Zhao et al., 2020). Exosomes have the potential to directly or indirectly promote axonal regrowth, protect neurons from degeneration, and support nerve regeneration processes such as remyelination (Bischoff et al., 2022; Kalluri and LeBleu, 2020; López-Leal et al., 2020; Zhao et al., 2020). Moreover, their delivery to nerves can help modulate inflammatory responses and reduce glial scar formation, facilitating the regeneration process (Wen et al., 2022). On the other hand, exosomes can enhance satellite cell activation and proliferation when directly or indirectly delivered to muscle tissues, leading to improved muscle regeneration and functional recovery (Ji et al., 2022; Wang et al., 2023). Additionally, exosome delivery to muscles can attenuate muscle inflammation and fibrosis, which are commonly observed following injury or denervation (Ji et al., 2022; Wang et al., 2023). In the context of motor endplate degeneration, which refers to the deterioration of the specialized connection between nerves and muscles, prolonged denervation can impair neuromuscular junction function of endplates and cause muscle atrophy. Local administration of exosomes to muscle tissue holds the potential to ameliorate endplate degeneration by supporting the preservation or regeneration of the endplate structure.

We found an interesting phenomenon in that the presence of exosomes in either autologous transplantation or treatment with BCM enhanced the repair effect of peripheral nerve defects. For example, the repair effect for the AUT+GAS^{EXO} group was better than that for the AUT group, and the EXO-BCM group and BCM+GAS^{EXO} group had better repair than did the BCM group (Figs. 2–4). These results are consistent with multiple other studies that showed a role for exosomes isolated from stem cells in promoting neuroprotection, neural regeneration, neural growth, neural flexibility, and improvement of neural dysfunction (Kalani et al., 2014; Khalatbary, 2021).

Our experiments showed that EXO-BCM is the best choice for repairing peripheral nerve defects after the autologous nerve transplantation (AUT group). With increasing time after surgery, the repair effect seen for the EXO-BCM group was nearly the same as that seen for autologous nerve repair (Figs. 2–4). In this study, we designed two methods using BCM together with exosomes. One method involved adding exosomes to the BCM (EXO-BCM group), while the other involved injecting exosomes into the gastrocnemius muscle after connecting the two ends of the severed sciatic nerve with BCM (BCM+GAS^{EXO} group). We then evaluated the two methods in terms of
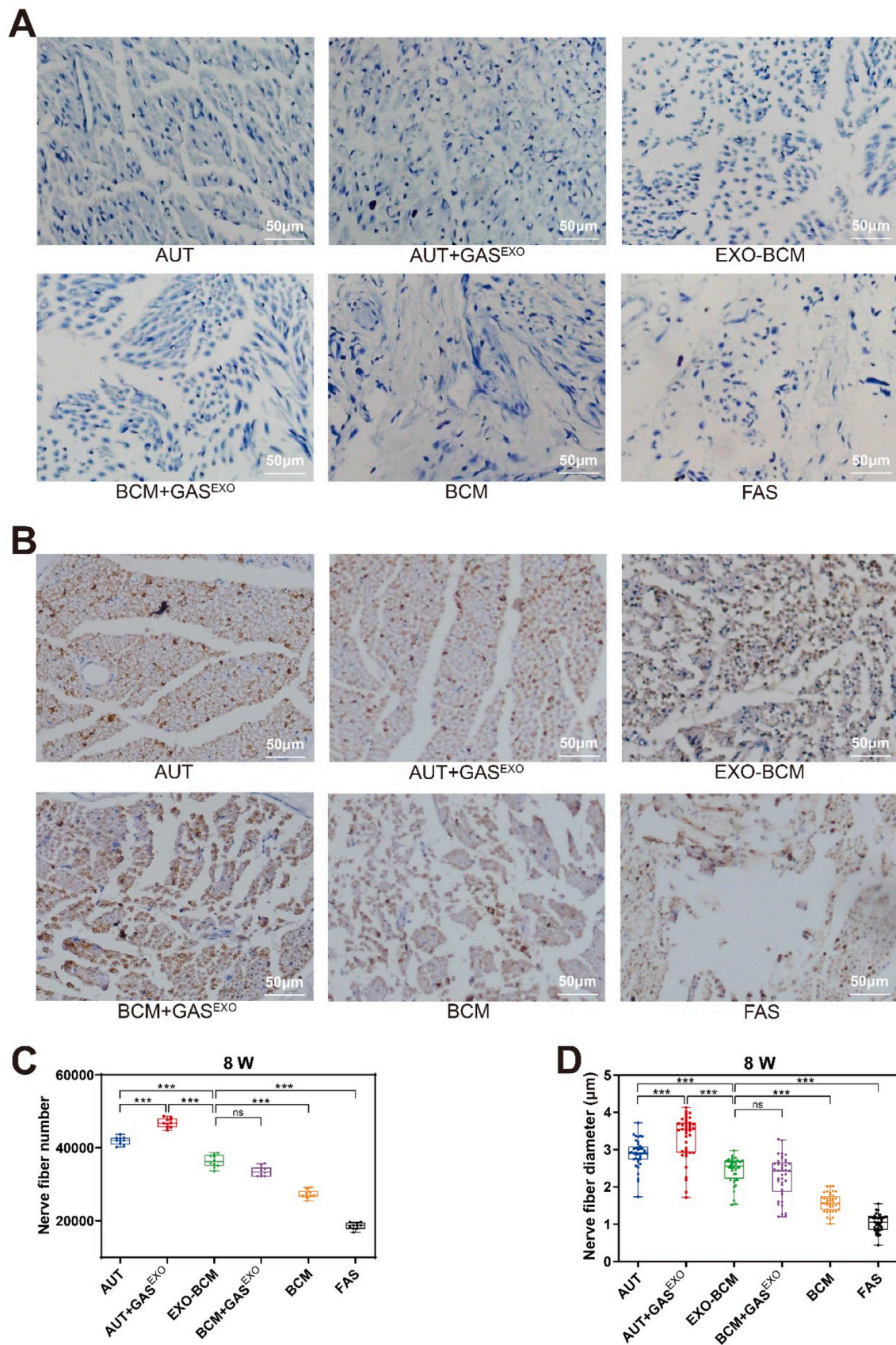
Fig. 4. Immunohistochemistry and morphometry of regenerated nerve fibers in rats in the different experimental groups. (A) Toluidine blue staining of regenerated nerve fiber sections. (B) 3,3'-diaminobenzidine staining and hemataoxylin staining of regenerated nerve fiber sections after incubation with S100 antibodies. Average (C) number and (D) average diameter of regenerated nerve fibers. n = 6 (A and B), n = 10 (C), n = 40 (D), * adjusted P values between 0.05 and 0.01, ** adjusted P values between 0.01 and 0.001, *** adjusted P values P < 0.001.

behavioral presentation and by measuring parameters such as SFI, PWTL, and quality and quantity of regenerated nerve fibers. The experimental results indicated an overall similar outcome for the EXO-BCM and BCM+GAS^{EXO} groups, with a slightly superior effect seen for the EXO-BCM group. With respect to obtaining bridging materials, EXO-BCM has an advantage over autologous transplantation in that obtaining EXO-BCM involves no secondary pain to the patient. Based on these results, the EXO-BCM group should be considered first from the perspective of reducing patient pain.

In summary, here we describe a method for repair peripheral nerve defects that involves a complex of BCM and exosome. This method could be valuable for cases in which autologous nerves cannot be obtained and may have broad applications for nerve defect repair. We are currently studying strategies for clinical development of this material.

Funding

CRediT authorship contribution statement

Conceptualization, X.N.Y. and R.J.F.; methodology, T.W.C.; software, T.W.C. and R.J.F.; validation, Y.B.H. and Y.R.W.; formal analysis, Q.P.Z.; investigation, R.R.; resources, X.D.C.; data curation, X.Y.B and P.L.N.; writing—original draft preparation, T.W.C. and L.F.L.; writing—review and editing, X.N.Y. and R.J.F.; visualization, T.W.C. and R.J.F.; supervision, Z.J.M. and Y.Q.L.; project administration, X.N.Y. and R.J.F.; funding acquisition, L.F.L., X.N.Y. and R.J.F. All authors have read and agreed to the published version of the manuscript.

Conflicts of interest

The authors declare no competing interests.

Acknowledgments

Appendix A. Supporting information

Supplementary data associated with this article can be found in the online version at doi:10.1016/j.ibneur.2023.09.009.

References

Bandeira, E., Oliveira, H., Silva, J.D., Menna-Barreto, R.F.S., Takyia, C.M., Suk, J.S., Witwer, K.W., Paulaitis, M.E., Hanes, J., Rocco, P.R.M., Morales, M.M., 2018. Therapeutic effects of adipose-tissue-derived mesenchymal stromal cells and their extracellular vesicles in experimental silicosis. Respir. Res. 19, 104.

Bischoff, J.P., Schulz, A., Morrison, H., 2022. The role of exosomes in intercellular and inter-organ communication of the peripheral nervous system. FEBS Lett. 596, 655–664.

de Medinaceli, L., Freed, W.J., Wyatt, R.J., 1982. An index of the functional condition of rat sciatic nerve based on measurements made from walking tracks. Exp. Neurol. 77, 634–643.

Dervan, A., Franchi, A., Almeida-Gonzalez, F.R., Dowling, J.K., Kwakyi, O.B., McCoy, C.E., O'Brien, F.J., Hibbitts, A., 2021. Biomaterial and therapeutic approaches for the manipulation of macrophage phenotype in peripheral and central nerve repair. Pharmaceutics 13.

Dubey, S., Mishra, R., Roy, P., Singh, R.P., 2021. 3-D macro/microporous-nanofibrous bacterial cellulose scaffolds seeded with BMP-2 preconditioned mesenchymal stem cells exhibit remarkable potential for bone tissue engineering. Int. J. Biol. Macromol. 167, 934–946.

Hazer, D.B., Bal, E., Nurlu, G., Benli, K., Balci, S., Ozturk, F., Hazer, B., 2013. In vivo application of poly-3-hydroxyoctanoate as peripheral nerve graft. J. Zhejiang Univ. Sci. B 14, 993–1003.

Hazer Rosberg, D.B., Hazer, B., Stenberg, L., Dahlin, L.B., 2021. Gold and cobalt oxide nanoparticles modified poly-propylene poly-ethylene glycol membranes in poly (epsilon-caprolactone) conduits enhance nerve regeneration in the sciatic nerve of healthy rats. Int. J. Mol. Sci. 22.

Hou, Y.J., Wang, X.Y., Yang, J., Zhu, R., Zhang, Z.R., Li, Y., 2018. Development and biocompatibility evaluation of biodegradable bacterial cellulose as a novel peripheral nerve scaffold. J. Biomed. Mater. Res. Part A 106, 1288–1298.

Ji, S., Ma, P., Cao, X., Wang, J., Yu, X., Luo, X., Lu, J., Hou, W., Zhang, Z., Yan, Y., Dong, Y., Wang, H., 2022. Myoblast-derived exosomes promote the repair and regeneration of injured skeletal muscle in mice. FEBS Open Bio 12, 2213–2226.

Kalani, A., Tyagi, A., Tyagi, N., 2014. Exosomes: mediators of neurodegeneration, neuroprotection and therapeutics. Mol. Neurobiol. 49, 590–600.

Kalluri, R., LeBleu, V.S., 2020. The biology, function, and biomedical applications of exosomes. Science 367, 640.

Khalatbary, A.R., 2021. Stem cell-derived exosomes as a cell free therapy against spinal cord injury. Tissue Cell 71, 101559.

Li, Y., Ma, Z., Ren, Y., Lu, D., Li, T., Li, W., Wang, J., Ma, H., Zhao, J., 2021. Tissue engineering strategies for peripheral nerve regeneration. Front. Neurol. 12, 768267.

López-Leal, R., Díaz-Viraqué, F., Catalán, R.J., Saquel, C., Enright, A., Iraola, G., Court, F. A., 2020. Schwann cell reprogramming into repair cells increases miRNA-21 expression in exosomes promoting axonal growth. J. Cell Sci. 133.

Lv, X., Feng, C., Liu, Y., Peng, X., Chen, S., Xiao, D., Wang, H., Li, Z., Xu, Y., Lu, M., 2018. A smart bilayered scaffold supporting keratinocytes and muscle cells in micro/nano-scale for urethral reconstruction. Theranostics 8, 3153–3163.

Meyer, C., Stenberg, L., Gonzalez-Perez, F., Wrobel, S., Ronchi, G., Udina, E., Suganuma, S., Geuna, S., Navarro, X., Dahlin, L.B., Grothe, C., Haastert-Talini, K., 2016. Chitosan-film enhanced chitosan nerve guides for long-distance regeneration of peripheral nerves. Biomaterials 76, 33–51.

Niu, Y., Chen, K.C., He, T., Yu, W., Huang, S., Xu, K., 2014. Scaffolds from block polyurethanes based on poly(varepsilon-caprolactone) (PCL) and poly(ethylene glycol) (PEG) for peripheral nerve regeneration. Biomaterials 35, 4266–4277.

Powell, R., Eleftheriadou, D., Kellaway, S., Phillips, J.B., 2021. Natural biomaterials as instructive engineered microenvironments that direct cellular function in peripheral nerve tissue engineering. Front. Bioeng. Biotechnol. 9, 674473.

Sakar, M., Korkusuz, P., Demirbilek, M., Cetinkaya, D.U., Arslan, S., Denkbas, E.B., Temucin, C.M., Bilgic, E., Hazer, D.B., Bozkurt, G., 2014. The effect of poly(3-hydroxybutyrate-co-3- hydroxyhexanoate) (PHBHHx) and human mesenchymal stem cell (hMSC) on axonal regeneration in experimental sciatic nerve damage. Int. J. Neurosci. 124, 685–696.

Samfors, S., Karlsson, K., Sundberg, J., Markstedt, K., Gatenholm, P., 2019. Biofabrication of bacterial nanocellulose scaffolds with complex vascular structure. Biofabrication 11.

Stumpf, T.R., Pertile, R.A., Rambo, C.R., Porto, L.M., 2013. Enriched glucose and dextrin mannitol-based media modulates fibroblast behavior on bacterial cellulose membranes. Mater. Sci. Eng. C Mater. Biol. Appl. 33, 4739–4745.

Stumpf, T.R., Tang, L., Kirkwood, K., Yang, X., Zhang, J., Cao, X., 2020. Production and evaluation of biosynthesized cellulose tubes as promising nerve guides for spinal cord injury treatment. J. Biomed. Mater. Res. A 108, 1380–1389.

Stumpf, T.R., Yang, X., Zhang, J., Cao, X., 2018. In situ and ex situ modifications of bacterial cellulose for applications in tissue engineering. Mater. Sci. Eng. C Mater. Biol. Appl. 82, 372–383.

Sun, A.X., Prest, T.A., Fowler, J.R., Brick, R.M., Gloss, K.M., Li, X., DeHart, M., Shen, H., Yang, G., Brown, B.N., Alexander, P.G., Tuan, R.S., 2019. Conduits harnessing spatially controlled cell-secreted neurotrophic factors improve peripheral nerve regeneration. Biomaterials 203, 86–95.

Wang, B., Lu, C.F., Liu, Z.Y., Han, S., Wei, P., Zhang, D.Y., Kou, Y.H., Jiang, B.G., 2022. Chitin scaffold combined with autologous small nerve repairs sciatic nerve defects. Neural Regen. Res. 17, 1106–1114.

Wang, Z., Yang, J., Sun, X., Sun, X., Yang, G., Shi, X., 2023. Exosome-mediated regulatory mechanisms in skeletal muscle: a narrative review. J. Zhejiang Univ. Sci. B 24, 1–14.

Wen, L., Wang, Y.D., Shen, D.F., Zheng, P.D., Tu, M.D., You, W.D., Zhu, Y.R., Wang, H., Feng, J.F., Yang, X.F., 2022. Exosomes derived from bone marrow mesenchymal stem cells inhibit neuroinflammation after traumatic brain injury. Neural Regen. Res. 17, 2717–2724.

Xun, X., Li, Y., Zhu, X., Zhang, Q., Lu, Y., Yang, Z., Wan, Y., Yao, F., Deng, X., Luo, H., 2021. Fabrication of robust, shape recoverable, macroporous bacterial cellulose scaffolds for cartilage tissue engineering. Macromol. Biosci. 21, e2100167.

Zhang, C., Cao, J.J., Zhao, S.Z., Luo, H.L., Yang, Z.W., Gama, M., Zhang, Q.C., Su, D., Wan, Y.Z., 2020. Biocompatibility evaluation of bacterial cellulose as a scaffold material for tissue-engineered corneal stroma. Cellulose 27, 2775–2784.

Zhao, J., Ding, Y., He, R., Huang, K., Liu, L., Jiang, C., Liu, Z., Wang, Y., Yan, X., Cao, F., Huang, X., Peng, Y., Ren, R., He, Y., Cui, T., Zhang, Q., Zhang, X., Liu, Q., Li, Y., Ma, Z., Yi, X., 2020. Dose-effect relationship and molecular mechanism by which BMSC-derived exosomes promote peripheral nerve regeneration after crush injury. Stem Cell Res. Ther. 11, 360.